

Recovery from Acid Rain in the Mississippi River Basin

Daniel J. Kozar^{1,2*}, Xiaoli Dong², Li Li¹

¹Department of Civil and Environmental Engineering, Pennsylvania State University, University Park, PA 16802

²Department of Environmental Science and Policy, University of California, Davis, CA 95616

Corresponding author: Daniel J. Kozar (djkozar@ucdavis.edu)

Key Points:

- Multiple lines of evidence suggest the recovery of water chemistry in streams and rivers from acid rain in the Mississippi River Basin
- Fertilizer use reduces pH in less affected areas, and increases cation export in all areas, reversing trends expected by acid rain recovery
- The signature by extended summer drought and elevated atmospheric CO₂ concentration under climate change is detected in water chemistry

Abstract

Acid rain has degraded environmental health since the Industrial Revolution. Legislative efforts have successfully reduced deposition rates, but recovery of affected ecosystems in the Mississippi River Basin (MRB) remains to be assessed. Combining analysis of temporal trends of indicative chemical species in streams and rivers with a Bayesian statistical model, we found strong evidence of reduced effect by acid rain on water chemistry; however, the effect by agricultural activities and climate change are intensifying. pH increased in the Eastern MRB, the historically more heavily affected region, and SO_4 loading decreased everywhere, suggesting recovery. Widespread fertilizer use, however, has likely accelerated carbonate weathering and water acidification. As a result, water became more acidic in western sites and annual divalent cation (DIV) load increased at all sites, showing statistically significant trends. Extended dry summers under climate change have likely contributed to SO_4 and DIV export via shale weathering in the basin, when the groundwater table drops. We also found evidence that, while not a significant contributor yet, ever increasing atmospheric CO_2 levels will likely add to cation export from the MRB in the future. Using long-term data over a large spatial scale, this study represents a comprehensive assessment of the recovery of water chemistry in river and stream ecosystems from acid rain in the Mississippi Basin, taking into consideration the entangled effects of agricultural activities, acid mine drainage, and extended droughts and elevated atmospheric CO_2 concentration under anthropogenic climate change.

Plain Language Summary

Human industrial activities have historically made rain more acidic, causing harm to the environment. American legislators passed laws in the late 20th century to decrease acid rain deposition. Surface loading of by-products of acid rain have decreased, but the question is: have rivers recovered? Some studies have looked at this, but there has not yet been an in-depth, comprehensive investigation in the Mississippi River Basin, which accounts for a large part of the continental United States. We found that areas

negatively affected by acid rain in the past showed recovery, but some trends seem to contradict expectations of recovery. We found that these contradictions are largely caused by fertilizer use in the Mississippi River Basin. Summer droughts also have some effect, but not as much as fertilizer. We also found that increased CO₂ levels in the atmosphere may, in the future, affect weathering, and therefore also the water chemistry in the streams and rivers of this basin.

1 Introduction

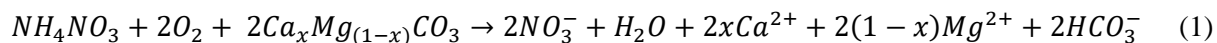
Acid rain, which arises from the release of sulfur dioxide (SO₂) and nitrogen oxides (NO_x) via electricity generation and transportation, as well as from other human activities (Likens et al., 1972), has impacted large parts of the Earth, especially North America, Europe, and Asia since the Industrial Revolution (Larssen et al., 2006; Stoddard et al., 1999). Beginning in the 1960s, and intensifying through the 1980s and 1990s, legislative action has been taken to limit its effects. The initial passage of the Clean Air Act (CAA) in the United States in 1963 was momentous, and efforts to mitigate acid rain deposition were further strengthened by amendments in 1990. The deposition rates of hydrogen ions have decreased drastically from consistently upwards of 0.5 kg/ha in 1985 to a few regions reaching rates of 0.2 kg/ha in 2016 in the Eastern USA (NADP, 2020). This leads to tantalizing questions about how Earth surface systems have responded to these reductions, and whether it is possible for Earth surface systems to fully recover to the pre-acid rain era. These large scale, unintended “experiments” are also a test of how well the effects of human perturbations can be absorbed by nature. Understanding these questions is particularly important as people have continuously and increasingly challenged the limits of the earth system with other human-induced impacts such as climate change, agriculture, and urbanization (Grimm et al., 2008).

Studies on Earth surface system response to reductions in acid deposition have primarily focused on soil and surface water. Studies on the recovery of surface waters have largely centered around streams of small forested catchments ranging from 1.78 to 820 km² (Clow & Mast, 1999; Likens et al., 1996; Majer et al., 2005; Marx et al., 2017; McHale et al., 2017). A few large scale studies analyzed recovery from acid rain at various locations in North America and Europe (Skjelkvåle et al., 2002; Stets et al., 2014; Stoddard et al., 1999). These studies generally concluded that stream sulfate (SO₄²⁻, hereafter referred to as SO₄) concentrations decreased as a result of reductions in wet deposition of SO₄ and hydrogen ions (H⁺) (Clow & Mast, 1999; Majer et al., 2005; Stoddard et al., 1999). Similar patterns of SO₄ reduction have been also reported by studies of lakes (Bouchard, 1997; Driscoll et al., 2003; Jeffries et al., 2000; Jeffries et al., 2003; Stoddard et al., 1999). The extent to which increase in pH correlates with SO₄ reduction, however, varies. For example, observed pH increases were not of the same magnitude of SO₄ decreases in the Hubbard Brook Experimental Forest (Likens et al., 1996). The pH trends were insignificant in relative magnitude compared to SO₄ trends in the Slavkov Forest, Czech Republic (Majer et al., 2005). This was largely attributed to pH buffering by the acid neutralizing capacity, which depends on multiple solutes from bedrock weathering (Bouchard, 1997). This is expected, as pH is not only determined by acid rain, but is also affected by local geology: for example, carbonate rocks provide more acid-buffering capacity than others.

Concentrations of cations, especially divalent cations (DIV), are expected to decrease as acid-rain deposition decreases and chemical weathering slows down (Likens et al., 1996). In addition, H⁺ deposition elevates concentrations of exchangeable aluminum, which is more readily adsorbed than calcium (Ca²⁺) and magnesium (Mg²⁺), therefore displacing these cations (Lawrence & Huntington, 1999; Walna et al., 1998). In fact, decline in concentrations of DIV has been observed in many streams and lakes alike as the acid deposition lessens (Bouchard, 1997; Jeffries et al., 2003; Majer et al., 2005; Waller et al., 2012). The observed relationship between SO₄ and cation concentrations, however, differs. In headwaters in the Northeastern United States, the decreases in SO₄ and in cation concentrations were

approximately the same (Clow & Mast, 1999). Stoddard et al. (1999) found that decreases in cation concentrations exceeded the relative magnitude of SO_4 decreases. This was attributed to the fact that weathering rates exceeded cation loss rates during times of high deposition (Stoddard et al., 1999). One potential confounding factor when considering cation concentrations is the atmospheric deposition of Ca^{2+} and Mg^{2+} . Mg^{2+} in rainfall decreased and Ca^{2+} increased from 1985 to 2016 in the United States (although Ca^{2+} in rain is < 1 mg/L, commonly < 0.5 mg/L) (NADP, 2020). Given that in-stream concentrations of Ca^{2+} are mostly > 20 mg/L (USGS, 2020), rainwater Ca^{2+} deposition is negligible in comparison to the concentration in streams. In summary, both geochemical theory and observations from previous studies suggest that signs of recovery will include increasing pH, decreasing SO_4 , and decreasing divalent cations (Ca^{2+} and Mg^{2+}), although the magnitudes of the changes may vary.

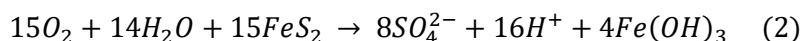
Additionally, pH is affected by other anthropogenic activities – notably the application of nitrogen-based fertilizers (Barnes & Raymond, 2009; Martin, 2017; Perrin et al., 2008; Thomson et al., 1993). The Mississippi River Basin (MRB) is historically 25-30% cultivated agriculture, and nutrient export from the Mississippi has attracted much focus as eutrophication is widespread in the Gulf of Mexico near the river outlet (Dodds, 2006; Rabalais et al., 2009). Application of nitrogen fertilizer (mostly NH_4NO_3) increases the release of cations such as Mg^{2+} and Ca^{2+} by accelerating the dissolution of carbonate (Eq. 1) (Perrin et al., 2008; Song et al., 2017):



Fertilizer application could also decrease the pH directly via nitrification (Perrin et al., 2008). This addition of H^+ may further accelerate carbonate weathering.

Changing climate can cause hydrologic changes, which further influence river biogeochemistry (Arnell 1999; Westmacott & Burn 1997). In particular, elongated droughts are expected to intensify in the future.

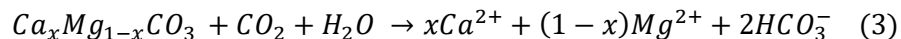
Summer droughts have been shown to lower the groundwater table, thus exposing shale to oxic conditions that would not be otherwise experienced (Crawford et al., 2019; Todd et al., 2012; Zhi et al., 2019). Shale formations are found throughout the MRB, therefore we can expect for drought induced shale oxidation to affect surface water chemistry. While no studies have assessed this mechanism in the MRB, drought induced shale oxidation has been observed to influence surface water chemistry in the Murray-Darling Basin in Australia (Mosley et al., 2014). Enhanced shale oxidation weathering has been observed to increase SO_4 and H^+ concentrations (Crawford et al., 2019) (Eq. 2)



The released H^+ could further drive rock weathering, releasing cations and increasing DIV.

Pyrite oxidation can occur via other pathways as well. Acid mine drainage (AMD) is the product of pyrite oxidation and is a common phenomenon in regions with mining activity (Akcil & Koldas, 2006). AMD is most commonly associated with coal mining (Qureshi et al., 2016). AMD has been observed in various regions of the MRB – particularly coal mining in Appalachia and the Rocky Mountains (USEIA, 2017). AMD and drought induced pyrite oxidation release the same chemical constituents (Eq. 2), but this reaction is induced via different pathways in each case. While oxygen is introduced via lowering of the water table in drought induced oxidation, oxygen is introduced via mining activities in the case of AMD (Akcil & Koldas, 2006). Open mines, above or under ground, and wastes from mines expose material to the atmosphere that would not otherwise be exposed. Bacteria also have been found to facilitate pyrite oxidation in many cases of AMD (Nordstrom, 2000). Just as with drought induced pyrite oxidation, AMD releases H^+ , SO_4 , and DIV.

Human activities have increased atmospheric CO₂ concentrations, which promotes the partial pressure of CO₂ ($p\text{CO}_2$) in soils, thus driving cation export from carbonate regions (Eq. 3) (Gaillardet et al., 2018; Lauerwald et al., 2013; Raymond & Cole, 2003; Raymond et al., 2013)



This process may significantly influence the carbon cycle, especially in the Anthropocene era (Gaillardet et al., 2018). The carbonate buffering system stabilizes pH in surface waters when large changes in pH are experienced, therefore it is expected that pH may have a positive correlation with carbonate related variables, such as percent area of karst in a basin or alkalinity. Additionally, unless shale weathering that oxidizes sulfides to sulfate is involved, we expect that dissolution of karst alone does not affect SO₄ concentrations.

This study addresses the following two questions: (1) is the Mississippi River Basin recovering from acid rain deposition? And (2) what factors influence the temporal trends observed of indicator chemical species (pH, SO₄, and DIV)? We use ~40-year long-term water chemical data collected from surface water of five tributaries and the outlet of the MRB. We first evaluate the temporal trends of pH and the annual flux of SO₄ and divalent cations (DIV) at various sites within the MRB. Second, we use a statistical model to test five hypotheses for drivers of the temporal trends (Fig. 1). We first hypothesize that the trends are driven by the recovery of acid rain (Fig. 1). Under this hypothesis, we expect a decrease in H⁺, SO₄, and DIV. We also hypothesize that the trends are affected by agricultural activities (Fig. 1). Under this hypothesis, we expect variables describing agricultural intensity to be negatively correlated with pH and positively correlated with DIV. We anticipate that SO₄ will not be correlated with agricultural predictors. Third, we hypothesize that observed trends are affected by a changing hydrological regime. With this hypothesis, we expect that SO₄ and H⁺ concentrations increase in elongated drought periods due to enhanced shale oxidation weathering. Additionally, we anticipate that

DIV will also have a negative relationship with discharge (Q), as the release of H^+ from shale oxidation (Eq. 2) can contribute to further carbonate weathering. **Fourth, we hypothesize that trends are driven by AMD. Under this hypothesis we expect H^+ , SO_4 , and DIV to be positively correlated with mining predictors.** Lastly, we hypothesize that the trends of the indicator chemical species might be driven by the rapidly-increasing atmospheric CO_2 (Fig. 1). Increased pCO_2 in soils can release cations via accelerated weathering (Eq. 3). However, pCO_2 in soils is typically orders of magnitudes higher than atmospheric pCO_2 , so we expect changes in atmospheric CO_2 are unlikely to make a significant effect (Karberg et al., 2005). Although increased atmospheric CO_2 levels cause ocean acidification (Doney et al., 2009), we do not expect that CO_2 will influence pH due to higher pCO_2 in the surface water than in the atmosphere – resulting in a riverine net loss of CO_2 (Choi et al., 1998). This concentration gradient results in an outgassing of $\sim 7.2 \text{ mmol m}^{-2} \text{ hr}^{-1}$ of CO_2 in the Lower Mississippi River (Reiman & Xu, 2019). Under this fifth hypothesis—that is, increased pCO_2 in the atmosphere accelerating weathering—we expect CO_2 is a significant predictor of DIV, but not of pH or SO_4 . Regardless of the mechanism, all hypotheses may influence the trends of chemicals through carbonate weathering (Fig. 1), hence we expect percent of karst cover of a catchment to be a significant mediating predictor of DIV. It is important to note that, most likely, multiple mechanisms are operating synergistically or antagonistically to influence the temporal trend of the indicator species in our study system.

2 Materials and Methods

2.1 Data Sources

We use historical water quality data from the United States Geological Survey (USGS) to evaluate the temporal trend of solutes indicative of acid rain recovery, including pH, SO_4 , and DIV (Table 1). This study primarily considers data from the outflow of the Mississippi River but also utilizes data from five tributary rivers into the Mississippi River (Fig. 2). By using data from the outflow site, the overall trend

throughout the entire basin that covers a large portion of the United States can be inferred. Data from tributary rivers capture spatial heterogeneity, as the catchments associated with these tributary rivers vary in land use, historical acid rain deposition rates, geology, and size.

2.1.1 Site Selection

A significant decrease in wet deposition of H^+ between 1985 and 2016 is observed in the eastern region of the MRB but a less drastic change occurs in the western region (NADP, 2020). The intensity of acid rain deposition experienced by each basin varied such that the trends in recovery may differ as well. While a direct comparison between east and west is not the driving force of this study, it is important to take into consideration the spatial heterogeneity of acid rain deposition. Comparing regions helps explain trends deviating from our hypotheses. We utilize two eastern tributaries - the Illinois River at Valley City, Illinois (ILLI-VC) and the Ohio River at Dam 53 near Grand Chain, Illinois (OHIO-GRCH). The western tributaries include the Mississippi River at Clinton, Iowa (MSSP-CL), the Iowa River at Wapello, Iowa (IOWA-WAP), as well as the Missouri River at Hermann, Missouri (MIZZ-HE). MSSP-OUT corresponds to the outflow site of this study (Table 1; Fig. 2).

Table 1. Metadata for sites in this study.

Site Name	Site Abbreviation	USGS Site ID	Basin Area (km ²)	Data Coverage Period	Region
Mississippi River at Clinton, IA	MSSP-CL	05420500	221,703	11/12/1974 – 12/1/2016	West
Iowa River at Wapello, IA	IOWA-WAP	05465500	32,375	11/10/1977 – 12/1/2016	West

Illinois River at Valley City, IL	ILLI-VC	05586100	69,264	12/12/1974 – 12/1/2016	East
Missouri River at Hermann, MO	MIZZ-HE	06934500	1,353,269	10/28/1969 – 12/1/2016	West
Ohio River at Dam 53 near Grand Chain, IL ¹	OHIO-GRCH	03612500	526,027	10/11/1972 – 12/1/2016	East
Mississippi River near St. Francisville, LA ²	MSSP-OUT	07373420	2,914,514	10/11/1974 - 8/14/2017	-

¹ Streamflow for this site was taken at the Ohio River at Metropolis, IL, USGS 03611500

²For this site, discharge is the sum of the outflows from Mississippi River at Tarbert Landing, LA (COE site 01100) and Old River Outflow Channel near Knox Landing, LA (COE 02600). This is to estimate a total flux from the river before the Old River Outflow Channel, where the Mississippi River splits and the Old River Outflow Channel joins the Atchafalaya River.

Due to divergence of the Mississippi River near the outflow into the Gulf of Mexico, this study utilizes water quality data from a site downstream of the divergence of the Mississippi River near St. Francisville, Louisiana (USGS 07373420). At this aforementioned split, the Atchafalaya River forms and the Mississippi River continues; the Old River Outflow Channel runs between these two rivers. The discharge we utilize is the summation of flow rates in the Mississippi River after the divergence (COE 01100) and in the Old River Outflow Channel (COE 02600) before it meets the Atchafalaya. The sum of flow at these two sites is considered the total outflow of the Mississippi River. The USGS and COE sites included in this study follow those of a USGS report on nitrate export into the Gulf of Mexico (Murphy et al., 2013).

2.1.2 Data on indicator solutes

The three indicator variables of interest are pH and the concentrations of SO₄ and DIV. DIV here is considered the total concentration of Ca²⁺ and Mg²⁺ (mg/L). Although acid rain contributes both SO₄ and

NO_x to the terrestrial landscape, we only use SO₄ as an indicator species as NO₃ is a common byproduct of agricultural activities (David et al., 2010). Mean daily concentrations of these chemical species were extracted from the USGS sites described above (Table 1).

2.1.3 Data for explanatory variables

We include two variables describing agricultural activities: the intensity of fertilizer application and percent cover of cultivated agriculture in the basin associated with each site, as these two metrics do not necessarily represent the same information. NO₃ concentration, as described above, is used as a proxy for fertilizer application (Eq. 1). Percent area of cultivated agriculture in the basin is determined for the years 2008-2017 using United States Department of Agriculture (USDA) Cropland Data Layer (CDL) maps (30-meter resolution) (USDA, 2020). **Coal production data is used to approximate the effect of AMD. While AMD can persist after coal extraction ends, via unclosed mines or waste, we neglect this effect as SO₄ export was shown to decrease after coal extraction ended even in one of the most affected rivers of the United States (Raymond & Oh, 2009). Annual coal production in each basin was estimated from United States Energy Information Administration (EIA) data (USEIA, 2017). This AMD data spans from 1983 to 2017. Mines located within the boundaries of the MRB were assigned to each respective sub-basin and were summed to calculate annual production by basin.** Annual global average CO₂ concentrations are taken from the National Oceanic and Atmospheric Administration (NOAA) Earth System Research Laboratories (ESRL) database (Tans & Keeling, 2020). We also determine the percent area of karst for each basin using the USGS Karst in the United States Map (Weary & Doctor, 2014). It is assumed that the percent karst in each basin does not change over time. Alkalinity is also used as an explanatory variable as it is a direct byproduct of carbonate weathering and contributes to acid neutralizing capacity. Lastly, discharge data from the USGS sites are included to account for the dependency of concentration on discharge.

2.2 Analysis

2.2.1 EGRET-WRTDS

The annual flow-weighted concentrations and fluxes of SO_4 , NO_3 , and DIV, as well as annual mean discharge (Q), are estimated using the USGS software program Exploration and Graphics for RivEr Trends (EGRET). EGRET is an R package for estimating long term changes in water quality developed by the USGS (Hirsch et al., 2010). This program uses input data from three sources: USGS water quality and hydrologic data, EPA STOrage and RETrieval (STORET) data, and user supplied data. EGRET utilizes the Weighted Regressions on Time, Discharge, and Season (WRTDS) method (Hirsch et al., 2010). WRTDS estimates discharge and concentration values for dates without values by assigning weight to the dates with missing data according to their temporal proximity to known values. WRTDS requires daily discharge records for the entire study period and is designed for large datasets, such as the one used in this study. The WRTDS model considers changes in water sampling techniques and frequencies. It uses water quality samples in a specific period to fit a statistical model to infer overall trends. Four variables are considered as affecting water quality, including long-term temporal trend, seasonal changes, discharge, and “random” causes. Seasonal changes affect geochemical behavior. Discharge is considered because concentration-discharge relationships affect export dynamics. In addition, there is also random noise and error in water quality data generated in observation, measurement, and data collection. The consideration of this random variation helps make more accurate predictions. WRTDS can be summarized by:

$$E[c] = w(Q, T) \quad (4)$$

where $E[c]$ is the estimation of the annual flux-weighted concentration, and $w(Q, T)$ means a function of discharge, Q , and time, T (annual), and takes the following form:

$$\ln(c) = \beta_0 + \beta_1 q + \beta_2 T + \beta_3 \sin(2\pi T) + \beta_4 \cos(2\pi T) + \varepsilon \quad (5)$$

where β 's are the regression coefficients, c is concentration [mg/L], q is $\ln(Q)$ [m³/s], T is time [years (decimal)], and ε is the error. The model uses this equation with provided data to infer gaps in the water quality record and to create long-term trends (Hirsch & De Cicco, 2015; Hirsch et al., 2010). Interested readers are referred to Hirsch et. al (2010) and Hirsch and De Cicco (2015) for more details. When using EGRET, it is important that all discharge data be included within the same time span as the water quality data (Hirsch & De Cicco, 2015).

2.2.2 Analysis of Temporal Trend

To evaluate the recovery from acid rain deposition using EGRET, only mean annual estimations of pH are used because pH cannot be evaluated as a load. For other solutes we use annual flux. Linear regression using flux and pH values as outcome variables against year is completed to evaluate the recovery over time from acid rain deposition. Linear regression using daily concentration estimations against year is used for comparison with daily concentration trends.

2.2.3 Bayesian Linear Models

To test the aforementioned hypotheses, three Bayesian models with varying slopes are constructed. A normal distribution is assumed for the data model:

$$OUT_i \sim Normal(\mu_i, \sigma) \quad (6)$$

where *OUT* is the daily value of outcome variable (here synonymous with indicator variable), either pH, SO₄ concentration, or DIV concentration (hence, three models); *i* is the site- and time (daily)-specific recordings. The mean model is described as:

$$\begin{aligned} \mu_i = & \alpha_{site(i),year(i)} + \beta_{NO3[site(i),year(i)]} NO3_i + \beta_{ALK[site(i),year(i)]} ALK_i + \beta_{AG[site(i),year(i)]} AG_i + \\ & \beta_{KARST[site(i),year(i)]} KARST_i + \beta_{PREV[site(i),year(i)]} PREV_i + \beta_{Q[site(i),year(i)]} Q_i + \\ & \beta_{AMD[site(i),year(i)]} AMD_i + \beta_{CO2[site(i),year(i)]} CO2_i \quad (7) \end{aligned}$$

$$\alpha_{site,year} \sim Normal(0,0.5) \quad (8)$$

$$\beta_{NO3[site,year]} \sim Normal(0,0.5) \quad (9)$$

$$\beta_{ALK[site,year]} \sim Normal(0,0.5) \quad (10)$$

$$\beta_{AG[site,year]} \sim Normal(0,0.5) \quad (11)$$

$$\beta_{KARST[site,year]} \sim Normal(0,0.5) \quad (12)$$

$$\beta_{PREV[site,year]} \sim Normal(0,0.5) \quad (13)$$

$$\beta_{Q[site,year]} \sim Normal(0,0.5) \quad (14)$$

$$\beta_{AMD[site,year]} \sim Normal(0,0.5) \quad (15)$$

$$\beta_{CO2[site,year]} \sim Normal(0,0.5) \quad (16)$$

$$\sigma \sim \exp(1) \quad (17)$$

All three models—one for each of the indicator species, pH, SO₄, and DIV—share the same model structure and same eight predictor variables. We include *Q* as a predictor variable to test the third hypothesis of this study (Fig. 1), and account for the effect of discharge on concentration. *AG* stands for agricultural land use within a watershed (between 0 and 1) and *KARST* stands for percent of karst cover within a watershed (between 0 and 1). *KARST* is constant over time for each site. As mentioned before, all sites lacked comprehensive *AG* data before 2008, therefore the data before 2008 are imputed. Daily NO₃

(mg/L) and alkalinity (mg/L as CaCO_3) data from the USGS are used for NO_3 and ALK respectively.

PREV corresponds to the previous outcome variable value in question, whether it be pH, SO_4 , or DIV.

AMD stands for the annual coal production (short tons). As mentioned before, AMD is only available after 1983. Therefore data for years before 1983 are imputed. CO_2 stands for mean annual atmospheric CO_2 concentration (ppm). Predictor data with annual values, such as CO_2 and AG , are assigned to all outcome variables corresponding to the same year.

All the predictor and outcome variables are normalized by z -scoring; therefore, slope parameters reflect the influence of one standard deviation in the predictor variable on the outcome variable, which facilitates comparison of relative effective size by different variables. Sensible weak normal-distribution priors are used for the coefficient parameters (Eqs. 8-16). The variance parameter (Eq. 6) is assumed to have an exponential distribution with a shape parameter of 1 (Eq. 17).

This model is solved using the “Just Another Gibbs Sampler” (*rjags*) in R (Plummer, 2019). *rjags* uses Markov Chain Monte Carlo (MCMC) sampling from the joint posterior distribution to estimate mean and Bayesian credible intervals of the parameters in the models. In this study, 95% credible intervals are used to determine statistical significance. Using MCMC we sample the posterior 3,000 times following a 500-count burn-in period using three chains. The model is then updated for another 6,000 times. The thinning rate on the model is 2 to eliminate autocorrelation in samples. A total of 3,750 effective samples are used to estimate the posterior distributions of parameters. \hat{r} values are checked to ensure all values are below 1.1, suggesting convergence of the model (Gelman et al., 2013). We derive site-specific effect by averaging the site- and year-specific parameters across all years. Similarly, for year-specific effect, we average the site- and year-specific parameter across all sites. The overall effect of a predictor variable is derived by averaging the site- and year-specific parameter across all years and all sites. From knowing when and where the significant relationships between variables occur, the aforementioned hypotheses can be tested.

3 Results

3.1 Temporal trend

The EGRET annual estimations and the daily data show a similar pattern for pH: it decreases at all three western sites, i.e., MSSP-CL ($p = 0.00$), IOWA-WAP ($p = 0.06$), and MIZZ-HE ($p = 0.00$), and increases at the two eastern sites, i.e., ILLI-VC ($p = 0.00$) and OHIO-GRCH ($p = 0.00$), over the study period. At the outflow site, pH also increases ($p = 0.00$) (Fig. 3a). All aforementioned p -values are for annual pH. For daily trends, $p = 0.00$ for all sites.

Annual flux of SO_4 decreases for all sites ($p = 0.00$) except for MIZZ-HE, which increases in time ($p = 0.00$) (Fig. 3b). At all sites in the study, except for MSSP-CL, daily SO_4 concentrations show a decreasing trend over the study period ($p = 0.00$ for all sites). At MSSP-CL, daily records show a slight increase in concentration. SO_4 flow normalized loads at the outflow site suggest that the MRB is experiencing a significant decrease in SO_4 loading overall.

EGRET estimations for annual DIV flux increase ($p = 0.00$) for all sites except for OHIO-GRCH (Fig. 3c). The negative trend at OHIO-GRCH is not statistically significant ($p = 0.10$). Daily concentration data show positive trends at all sites ($p = 0.00$) except for IOWA-WAP, which shows a decreasing trend. DIV flow normalized load at MSSP-OUT shows that DIV loading is significantly increasing over time in the MRB.

3.2 Bayesian Linear Models

3.2.1 pH

pH is significantly influenced by alkalinity and NO_3 , as well as discharge (Fig. 4). The influence of alkalinity and NO_3 is largely site specific rather than year specific. The effect of alkalinity displays positive statistical significance in 3 of the 44 years in the study period – 2008, 2014, and 2017. In comparison to this, when averaging over years, all sites except IOWA-WAP show positive influence of alkalinity on pH, with three of the six sites showing significance – ILLI-VC, MIZZ-HE, and MSSP-OUT. Despite not being statistically significant, the other two sites showing positive influence, MSSP-CL and OHIO-GRCH, show similar β_{ALK} values. The overall effect size of alkalinity is 0.08 and is statistically significant. The effect of NO_3 on pH shows similar patterns. Averaging across sites, β_{NO_3} is significant only in 2012 and 2015. The three western sites in this study show negative statistical significance of NO_3 when averaged across years. The three other sites all show negative influence, although none is statistically significant. There is an overall significantly negative effect of -0.07 by NO_3 on pH. The effect of atmospheric CO_2 is significant only in 1982 (averaging over all sites) and only at ILLI-VC (averaging over all years) (Fig. 4), with its overall effect not significant. β_Q at all sites, except for OHIO-GRCH, are significantly negative. Discharge shows the most negative influence at the site IOWA-WAP, with a value of -0.64. Discharge shows significantly negative influence in 22 out of 44 years, while all years showed negative mean influence. The overall effect of discharge on pH is statistically significant with a mean value of -0.31. The rest of the explanatory variables are largely not significant predictors of pH. The intercepts, α , are mostly negative, but not significant. **β_{AMD} is statistically insignificant at any site or any year, but shows a slightly negative effect. When averaged across years and sites β_{AMD} has an overall mean of -0.10.** The coefficients for cropland cover, β_{AG} , and for karst cover, β_{KARST} , are largely

positive, but not significant. Previous pH values show a positive influence but exhibit no significance when averaged over sites or years.

3.2.2 SO_4

Posterior distributions of coefficients from the SO_4 model show that SO_4 is largely determined by alkalinity and discharge, and secondary determined by NO_3 (Fig. 5). The effect of alkalinity, β_{ALK} , averaging across sites, shows positive statistical significance in all years except for 2012. When averaging across years, β_{ALK} is statistically significant for all sites. The overall effect of alkalinity is significantly positive with a mean of 0.24. The effect of discharge is significantly negative at all sites except for MSSP-CL. Discharge has the strongest effect on SO_4 at IOWA-WAP. When averaging across sites, β_Q is significant for all years except eleven. The overall effect of Q is significant with a mean value of -0.43. The effect of NO_3 only is significant in 2008 and 2011. When averaging over the study period, the effect of NO_3 is significant at IOWA-WAP and MIZZ-HE. The overall value of β_{NO3} is -0.04 and is statistically insignificant. **The effect of AMD, β_{AMD} , is insignificant for all years and all sites and shows a slightly positive influence on SO_4 . The overall effect size, averaged over all years and sites, β_{AMD} is 0.08.** The effect of atmospheric CO_2 , β_{CO2} , is significant at MSSP-OUT. As MSSP-OUT acts as a site integrating all processes for all of the basin, CO_2 in the atmosphere influences the basin as a whole even though it may not for individual sites. The overall effect of atmospheric CO_2 —that is, β_{CO2} averaged over all years and all sites—is significantly negative. Intercepts are not significant for any year or any site but are largely negative with a mean of -0.07. β_{AG} and β_{KARST} show no statistical significance for any year or site.

3.2.3 DIV

The variables that explain most of the variation in DIV are alkalinity, karst cover, Q , and NO_3 . The effect of alkalinity on DIV is statistically significant for all years and all sites, with an overall effect size of 0.53. When averaged over sites, the effect size of alkalinity increases over the study period (Fig. 6). The effect of karst cover is significantly positive in all years and at all sites, with a mean of 1.30, much larger than other covariates. β_Q is significantly negative correlation overall and at all sites when averaged across years. The effect of discharge on DIV is significantly negative in 20 out of 44 years, when averaged across sites. Fertilizer application exhibits a significantly positive effect on DIV in all years and all sites, with an overall mean effect of 0.25 (Fig. 6). The sites with the highest β_{NO_3} are ILLI-VC, MSSP-CL, and OHIO-GRCH with mean values of 0.27, 0.28, and 0.29, respectively. **β_{AMD} is statistically insignificant for all years and all sites and shows a slightly positive influence on DIV. When averaged over all years and sites, β_{AMD} is 0.03, although not significant.** Atmospheric CO_2 does not show statistical significance for any year or site, although from visual inspection, mean effect sizes seem to increase over the study period (Fig. 6). Lastly, intercepts for the DIV model show statistically significant negative values in all years and at all sites. Intercepts are consistently negative across sites but exhibit slightly greater magnitude for the eastern sites (ILLI-VC and OHIO-GRCH) compared to the western sites.

4 Discussion

The majority of existing studies assessing legacy effects by acid-rain deposition have been conducted on small scale catchments (Clow & Mast, 1999; Likens et al., 1996; Majer et al., 2005; Marx et al., 2017; McHale et al., 2017). Large-scale studies are still limited. Stoddard et al. (1999) investigated in-stream recovery of acid rain deposition at 205 streams and lakes throughout the northeastern United States and Europe between 1980 and 1995. They found evidence that efforts to reduce acid-rain were successful. However, the study by Stoddard et al. (1999), as well as similar large-scale studies carried out in

comparable regions (e.g., Skjelkvåle et al., 2002), were conducted on a relatively short timescale due to the proximity in time to the efforts to reduce acid rain. A large scale study throughout the United States inferred recovery from acid rain from decreasing ratios between cation and alkalinity concentrations (Stets et al., 2014). Another large scale study between 1990 and 2008 found evidence of recovery but did not consider any sites in the American Midwest (Garmo et al., 2014). Here, we analyzed long-term temporal trends of a set of solutes relevant to acid rain deposition and tested multiple hypotheses in explaining the trends. By teasing apart confounding drivers, we conclude with more confidence that legislative efforts to reduce acid rain have shown recovery in water chemical constituents. We find strong evidence to support recovery from acid rain reflected in the reduction of H^+ , SO_4 and DIV load and concentrations in rivers at the MRB, especially at the eastern region of the river basin. In the western region, other factors in addition to reduced acid rain deposition come into play, including changing hydrological regimes and fertilizer use. These factors lead to increased DIV and SO_4 export, reversing the decreasing trend expected by acid rain recovery. Although our results do not prove broad significance of the effect of atmospheric CO_2 on freshwater geochemistry, there are signs of potentially intensifying effects in the future.

4.1 Evidence of Recovery from Acid Rain

Results of this study clearly suggest the recovery of the MRB from acid rain deposition, as shown in temporal trends of both pH and SO_4 at the outlet of MRB (Fig. 3), consistent with what has been reported in previous studies. An investigation using data from sites throughout Europe and northeastern North America observed increasing pH at impaired sites following reductions in acid rain (Garmo et al., 2014). Increasing pH was also observed in many forested catchments (e.g., Driscoll et al., 2003; Likens et al., 1996; Waller et al., 2012). As industrial activities contributing to acid rain decrease, SO_4 in surface water has been known to decrease (Driscoll et al., 2003; Likens et al., 1996; Stoddard et al., 1999), consistent with what we found in our study, except for the site of MIZZ-HE, where flow normalized SO_4 load

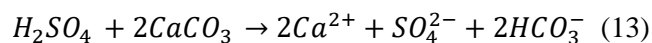
increased over the study period. This temporal trend is likely caused by shale weathering enhanced by longer dry periods under climate change, which we discuss in Section 4.3 below.

A spatial distinction between east and west is in pH, as eastern sites showed an increasing trend while pH in western sites decreased over time. Decreasing pH at western sites is not likely a sign of a legacy effect by acid rain; instead, more acidic water at the western sites is likely caused by fertilizer use. In addition to contributing to carbonate dissolution, nitrogen-based fertilizers can release H^+ (Eq. 1). The model results show that fertilizer application has a significantly negative effect on pH at the three western sites, while at the two eastern sites, the effect is not significant. However, fertilizer use is also widespread in the Ohio River Basin in the states of Ohio and Indiana (Potter et al., 2010). The difference in the response of pH to fertilizer application likely reflects the relative difference in the severity of historic acid rain deposition between the east and the west regions. Areas west of Illinois and Missouri experienced less acid rain deposition before the passing of the CAA and its amendments (NADP, 2020). The pH in the 1970s at the eastern sites was much lower than that at the western sites (Fig. 3). While both regions recover from the acid rain, the signature of pH is dominated by intensified fertilizer application in the west MRB, while in the east, it is dominated by the effect of recovery.

It is widely accepted that acid-rain deposition results in the release of divalent cations (Clow & Mast, 1999; Likens et al., 1996). Reduction in DIV export is often observed as acid rain deposition becomes weaker (Clow & Mast, 1999; Driscoll et al., 2003; Jeffries et al., 2000; Jeffries et al., 2003). In fact, it has been observed that DIV reductions exceeded SO_4 reductions following acid-rain legislation (Skjelkvåle et al., 2002). A study on small watersheds in the Catskill Mountains reported that decreased acid-rain deposition leads to lower weathering rates and aquatic cation concentrations (McHale et al., 2017). In our study, however, only the most eastern-situated basin, the Ohio River Basin, showed a decrease in flux ($p = 0.10$) (Fig. 3), while DIV flux increased significantly at the rest of sites. These temporal trends in DIV

suggest that DIV export might be driven by a separate process from reduced acid rain deposition. We discuss this in the next section on the effect of agriculture.

The statistical model in this study shows that the most reliable predictors for variation in SO_4 are alkalinity, NO_3 , Q and CO_2 . The positive relationship between alkalinity and SO_4 is likely a result from dissolution via acid rain deposition (Eq. 13), as alkalinity and SO_4 are products of the same process (Reddy et al., 1986).



Given the strong evidence showing the reduction of acid rain deposition in this study, one may be curious as how these can be related if the process that drives them is declining. Although acid rain deposition has declined over the years, it is not completely gone. As of 2014, wet deposition rates of SO_4 in the Eastern United States were estimated to be 20% of peak deposition rates (Rice et al., 2014). Sulfur dioxide emissions in the United States only decreased 40% between 1980 and 1999 (Menz & Seip, 2004), so although deposition rates have been declining for decades (Fig. 3), the relationship between SO_4 and alkalinity should remain (Fig. 5). Fertilizer application shows a negative influence on SO_4 , but in much smaller magnitude at a mean of -0.04 compared to a mean effect size of 0.24 by alkalinity (Fig. 5). In addition to showing lesser magnitude, the effect of fertilizer is only significant at two sites - IOWA-WAP and MIZZ-HE. We did not expect fertilizer to influence SO_4 . We suspect that the significant relationship between SO_4 and NO_3 is merely a statistical correlation: as few processes influence SO_4 concentration in streams and rivers, the decline of SO_4 coincides with the increase of fertilizer application in the long term, which results in the spurious correlation. Similarly, atmospheric CO_2 showed a significant negative influence on SO_4 when averaged across both years and sites and as well as at the outflow site itself. We believe this is also a result of spurious correlation, and is discussed in more detail in Section 4.4. The observed relationship between SO_4 and Q in the model is likely caused by drought related weathering,

further discussed in Section 4.3 below. Overall, results from both temporal analysis and the statistical models suggest that, in the MRB, acid rain deposition as well as its biogeochemical consequences are declining, although the signatures are entangled by influences from other various processes related to human activities and climate change.

4.2 Influence of Agriculture

The biogeochemical influence of agricultural activities in the MRB has been a point of focus for many years as it is the primary contributor to eutrophication in the Gulf of Mexico (Thrash et al., 2017). Although nitrogen fertilizer use in the United States has stagnated, the MRB remains one of the most intensely fertilized regions of the world (Lu, 2017; Potter et al., 2010). Fertilizers are known to increase cation export by accelerating weathering of carbonate (Perrin et al., 2008; Song et al., 2017). Results from the statistical model of DIV suggest that widespread fertilizer use in the MRB has likely contributed to the increasing DIV trends (Fig. 6). Moreover, we notice a mild increase in the effect of fertilizer application on DIV, especially after 2000 (Fig. 6), which might indicate a potential buildup consequence. If this is so, we predict that cation export will continue long after any mitigation efforts on fertilizer application in the MRB (Barak et al., 1997).

Our inference of the effect of fertilizer on surface water geochemistry is corroborated by the significantly negative relationship between NO_3 and pH (Eq. 1; Fig. 4). This result echoes findings on the effects of nitrogen-based fertilizers on soil pH (Thomson et al., 1993), because the application of nitrogen fertilizers induces nitrification, which produces H^+ as a byproduct (Perrin et al., 2008). Although this study focuses on aquatic constituents, if fertilizers such as NH_4NO_3 can decrease soil pH, surface and shallow subsurface runoff will consequently decrease pH in streams and rivers.

Furthermore, as alkalinity and karst are hypothesized to be central mediating variables in the mechanisms of fertilizer affecting H^+ and DIV (Fig. 1), we expect karst cover and alkalinity to be significant predictors of DIV. This is supported by our model result (Figs. 4 and 6). Alkalinity showed significant influence on pH and DIV, with stronger effect on DIV and weaker effect on pH (Figs. 4-6). The weak relationship with pH is expected as alkalinity represents the extent to which a parcel of water can resist changes in pH. DIV and alkalinity can be increased by elevated atmospheric CO_2 and/or intensified fertilizer application, both of which enhance weathering of carbonate rocks. We observe a stronger correlation between fertilizers and DIV in comparison to CO_2 and DIV (Fig. 6). This suggests that in the MRB, alkalinity is likely largely driven by carbonate weathering accelerated by fertilizer application, which further influences other water chemistry (Figs. 4-6).

4.3 Drought Driven Weathering

Climatic variations commonly influence hydrological flow regimes in surface waters (Arnell 1999), which can influence rock weathering and solute concentrations. The effect of discharge on SO_4 are significantly negative at all sites, except for MSSP-CL (Fig. 5). Discharge also has a significantly negative effect on DIV at all sites (Fig. 6). In particular, strong effect of discharge on SO_4 and DIV are found in both MIZZ-HE and ILLI-VC sites (Figs. 5–6). These two sites drain water from shale-containing rocks (Martin, 2017; Moosdorf et al., 2010) and SO_4 is produced by the oxidation of shale that contains sulfide (Eq. 2). It has been proposed recently that dry summers and extended drought periods can lower the groundwater table and expose deeper shale rock to O_2 , leading to shale oxidation that produces SO_4 (Crawford et al., 2019; Todd et al., 2012). This oxidation reaction releases H^+ , which, in turn, can facilitate carbonate dissolution and elevate DIV (Crawford et al., 2019). In wetter periods with relatively higher groundwater table, shale oxidation is reduced, as SO_4 and DIV at depth enter rivers via subsurface runoff and become diluted under high discharge (Zhi et al., 2019).

As shale oxidation releases H^+ , we expected a significant positive relationship between discharge and pH (Hemingway et al., 2020). However, instead, the model result indicates a negative correlation, *i.e.*, drier conditions are featured with less acidic surface flow. We infer that it might have to do with the dual effects of discharge on pH. While droughts induce accelerated shale weathering, releasing higher H^+ , they also change the relative contribution of different water sources to river surface flow (van Vliet & Zwolsman, 2008). During dry periods, a higher proportion of river flow is contributed by baseflow, instead of by runoff via precipitation. Historically, pH of rainfall in the U.S. ranges between 4.5 and 6.4 (Wisniewski & Keitz, 1983), while the pH in streams and rivers are > 7.0 (Fig. 3). Therefore, if the net effect of discharge on pH is negative (Fig. 4), it suggests a dominant effect of physical dilution/concentration by discharge. Since (1) the total effect of discharge—including its direct dilution/concentration effect and indirect effect on shale weathering—on H^+ , SO_4 , and DIV is about twice the effect size of fertilizer application (Figs. 4-6), and (2) the total effect of discharge is dominated by the direct effect of physical dilution/concentration, we can infer that the effect size by fertilizer use is greater than the effect of shale weathering on water chemistry in the Mississippi Basin. Fertilizer application is the primary cause of the deviation of the DIV and pH trends from the trend expected by acid rain recovery.

4.4 AMD

AMD is a serious environmental concern in areas of historic intensive coal mining, and is estimated to have impaired thousands of kilometers of surface waters in the United States as of 1990 (Herlihy et al., 1990). AMD is commonly associated with the Appalachian region, specifically Pennsylvania, Ohio, and West Virginia (USEIA, 2017). Most of Pennsylvania drains into the Chesapeake Bay, rather than into the Gulf of Mexico – possibly limiting the impact of AMD on the MRB. Certainly there are other regions of intensive coal mining elsewhere in the MRB – namely Wyoming, Illinois, and Indiana (USEIA, 2017). Considering the locations of historic coal mining, AMD was expected

to exhibit most effect on the basins of the Ohio River (OHIO-GRCH) and the Missouri River (MIZZ-HE). However, the effect of AMD on the constituents of interest in this study was not significant in any of the sites we examined. Despite this, the overall direction of the trends did tend towards expectations; coal production tended to have a slightly negative effect on pH, and slightly positive effects on SO₄ and DIV. Our findings suggest that AMD does not influence aquatic geochemistry on large scales in comparison to other influences such as agriculture or atmospheric deposition. However, this does not negate the need to remediate AMD affected areas as the local effects of AMD are often severe (Gray, 1997).

4.5 Atmospheric CO₂

Industrial activities have increased CO₂ in the atmosphere globally. Aside from contributing to warming, elevated CO₂ is known to affect terrestrial and ocean biogeochemistry (Doney et al., 2009; Doherty et al., 2010). Elevated atmospheric CO₂ causes ocean acidification via direct contact with the water surface (Doney et al., 2009). In streams and rivers, however, due to the negative partial pressure gradient between surface waters and the atmosphere, often it is not expected for atmospheric CO₂ to influence constituents in freshwater systems via the water-air interface directly (Neal & Whitehead, 1988). In terrestrial ecosystems, soil pCO₂ is often much larger than that of the atmosphere (Karberg et al., 2005). We therefore expected that atmospheric CO₂ changes would not affect the indicator species in this study. We find that in general atmospheric CO₂ indeed does not show statistically significant effect on the indicator constituents. CO₂ shows a statistically significant negative correlation with SO₄ at the outflow site, MSSP-OUT, as well as for the overall effect (Fig. 5). We suspect that this significant correlation is due to the coincidence of monotonic increasing atmospheric CO₂ in the past few decades and the decreasing trend of SO₄ in water caused by reduction of acid rain deposition (IJC, 2014; Tans & Keeling, 2020). If CO₂ changes were to drive dissolution, CO₂ concentration and SO₄ concentration would be positively related.

While $p\text{CO}_2$ in soils is usually much higher than atmospheric CO_2 , it has been shown that soil $p\text{CO}_2$ is sensitive to atmospheric CO_2 (Gaillardet et al., 2018; Karberg et al., 2005). Therefore, with the drastic increase of CO_2 concentration since the Industrial Revolution, we expect that $p\text{CO}_2$ in air may eventually significantly affect the weathering rate of carbonates, especially in places where soil cover is shallow and/or carbonate bedrock is exposed. In our study, CO_2 does not significantly influence DIV export overall using a 95% credible interval, but is significant with an 80% credible interval, indicating the potential importance of $p\text{CO}_2$. Additionally, we find that the effect size increases over years with a slope of +0.004 standard scores per year (Fig. 6). As atmospheric CO_2 further increases due to fossil fuel combustion, this upward trend of the mean effect size is very likely to continue in the near future. Therefore, it might be reasonable to expect that atmospheric CO_2 will be an important variable influence on DIV in the near future (Fig. 6). Currently, however, the mean value of β_{CO_2} on DIV is 0.04, in comparison to 0.24 by fertilizer, suggesting that the influence of agricultural activities in the MRB on DIV at present is about 6 times greater than that of CO_2 .

5 Conclusions

Multiple lines of evidence from our study indicate that legislative efforts to reduce acid rain deposition in the United States have resulted in recovery of freshwater systems in the MRB, although it is not obvious overwhelmed by geochemical signatures by climate change and anthropogenic activities. The extent of recovery is heterogeneous in space, however, due to the heterogeneity in the degree of the impact by acid rain historically. A rise in pH levels is seen in heavily affected eastern sites, while negative trends are experienced in historically less affected sites in the western region of the MRB. With the recovery of aquatic systems from acid rain deposition, we find the intensifying effect on the surface water geochemistry to be caused by agricultural activities, in particular, the widespread use of fertilizers in the basin. Longer and intensifying drought periods under climate change are observed to increase

concentrations of SO_4 and DIV to the MRB, due to the effect on accelerated shale weathering when the groundwater table is lowered. However, the effect of shale weathering on SO_4 and DIV is not as strong as the effect of decreased deposition and fertilizer use. Signals of elevated atmospheric CO_2 in freshwater ecosystems remain weak, but there is evidence from our study that it might become an increasingly important driver in affecting aquatic geochemistry. This study represents a comprehensive assessment of the recovery of aquatic ecosystem geochemistry from acid rain in the Mississippi Basin, by effectively disentangling effects from multiple causes.

Acknowledgments, Samples, and Data

The research is funded by the U.S. Department of Energy (DOE) Subsurface Biogeochemical Research (SBR) program (DE-SC0016221) awarded to LL. DJK is supported by Graduate Fellowship with the Hydrologic Sciences Graduate Group at the University of California, Davis. The authors are grateful for helpful comments from Dr. Mark Klima at Pennsylvania State University on the earlier versions of this work.

The data used in this study are available in the following in-text citations: USGS, 2020, Weary & Doctor, 2014, Tans & Keeling, 2020, USEIA, 2017 and USDA, 2020.

Figure Captions

Figure 1: Conceptual diagram showing the five hypothesized mechanisms to influence the observed temporal trends of aquatic DIV, H^+ , and SO_4 in the MRB. Outcome variables (indicator species) are shown in circles. The processes (drivers) corresponding to the five hypotheses are shown in colored rectangles. Karst is shown in a grey rectangle with a dashed outline as it is a mediating variable shared by the five mechanisms to influence DIV.

Figure 2: Locations of USGS sites used in this study with corresponding influent basins in relation to contiguous United States. See Table 1 for site abbreviations.

Figure 3: Temporal trends of a) pH, b) annual sulfate (SO_4), and c) annual divalent cation (DIV) at each site according to mean annual estimates from EGRET. p -values of the annual trends are given in each subplot with the direction of overall trend denoted by an arrow. Upwards facing arrows correspond to positive trends while downwards facing arrows correspond to negative trends.

Figure 4: Whisker plots of effect size of alkalinity, fertilizer application (approximated by NO_3), atmospheric CO_2 , and discharge (Q) on pH. Parameters are either averaged by year (a), by site (b), or by both (c). When the 95% credible intervals do not contain 0, it means the effect is statistically significant. For site-specific parameters Western sites are shown with circular markers, Eastern sites are shown with square markers, and the outflow site is shown with a diamond marker.

Figure 5: Whisker plots of the effect size of alkalinity, fertilizer application (approximated by NO_3), atmospheric CO_2 , and discharge (Q) on SO_4 concentration. Parameters are either averaged by year (a), by site (b), or by both (c). When the 95% credible intervals do not contain 0, it means the effect is statistically significant. For site specific parameters Western sites are shown with circular markers, Eastern sites are shown with square markers, and the outflow site is shown with a diamond marker.

Figure 6: Model parameters α (intercept), β_{ALK} (coefficient for alkalinity), β_{NO_3} (coefficient of NO_3), β_{CO_2} (coefficient of atmospheric CO_2), β_Q (coefficient for discharge) and β_{KARST} (coefficient for karst cover in a basin) for the DIV model by year (a), site (b), and overall (c). β_{KARST} values are higher than the others in magnitude so are on a different scale to allow sufficient visual representation of the other five parameters. β_{KARST} is under a black line to denote a different vertical scale. When the 95% credible intervals do not contain 0, it means the effect is statistically significant. For site specific parameters Western sites are shown with circular markers, Eastern sites are shown with square markers, and the outflow site is shown with a diamond marker.

References

- Akcil, A., & Koldas, S. (2006). Acid Mine Drainage (AMD): Causes, treatment and case studies. *Journal of Cleaner Production*, 14(12-13), 1139-1145. doi:10.1016/j.jclepro.2004.09.006
- Arnell, N.W. (1999). The effect of climate change on hydrological regimes in Europe: a continental perspective. *Global Environmental Change*, 9, 5-23. [https://doi.org/10.1016/S0959-3780\(98\)00015-6](https://doi.org/10.1016/S0959-3780(98)00015-6)
- Barak, P., Jobe, B. O., Krueger, A. R., Peterson, L. A., & Laird, D. A. (1997). Effects of long-term soil acidification due to nitrogen fertilizer inputs in Wisconsin. *Plant and Soil*, 197, 61–69. <https://doi.org/10.1023/A:1004297607070>
- Barnes, R.T., & Raymond, P.A. (2009). The contribution of agricultural and urban activities to inorganic carbon fluxes within temperate watersheds. *Chemical Geology*, 266(3), 318-327. <https://doi.org/10.1016/j.chemgeo.2009.06.018>
- Bouchard, A. (1997). Recent lake acidification and recovery trends in southern Quebec, Canada. *Water, Air, and Soil Pollution*, 94, 225–245. <https://doi.org/10.1007/BF02406060>
- Choi, J., Hulseapple, S. M., Conklin, M. H., & Harvey, J. W. (1998). Modeling CO₂ degassing and pH in a stream-aquifer system. *Journal of Hydrology*, 209(1–4), 297–310. [https://doi.org/10.1016/S0022-1694\(98\)00093-6](https://doi.org/10.1016/S0022-1694(98)00093-6)
- Clow, W., & Mast, M. A. (1999). Long-term trends in stream water and precipitation chemistry at five headwater basins in the northeastern United States. *Water Resources Research*, 35(2), 541–554. <https://doi.org/10.1029/1998WR900050>
- Crawford, J.Y., Hinckley, E.S., Litaor, M.I., Brahney, J., & Neff, J.C. (2019) Evidence for accelerated weathering and sulfate export in high alpine environments. *Environmental Research Letters*, 14, 1-9. <https://doi.org/10.1088/1748-9326/ab5d9c>
- David, M. B., Drinkwater, L. E. & McIsaac, G. F. (2010). Sources of Nitrate Yields in the Mississippi River Basin. *Journal of Environmental Quality*, 39, 1657–1667. <https://doi.org/10.2134/jeq2010.0115>
- Dodds, W. K. (2006). Nutrients and the “dead zone”: The link between nutrient ratios and dissolved oxygen in the northern Gulf of Mexico. *Frontiers in Ecology and the Environment*, 4(4), 211–217. [https://doi.org/10.1890/1540-9295\(2006\)004\[0211:NATDZT\]2.0.CO;2](https://doi.org/10.1890/1540-9295(2006)004[0211:NATDZT]2.0.CO;2)
- Doherty, R. M., Sitch, S., Smith, B., Lewis, S. L., & Thornton, P. K. (2010). Implications of future climate and atmospheric CO₂ content for regional biogeochemistry, biogeography and ecosystem services across East

- 738 Africa. *Global Change Biology*, 16, 617–640. <https://doi.org/10.1111/j.1365-2486.2009.01997.x>
- 739 Doney, S. C., Fabry, V. J., Feely, R. A., & Kleypas, J. A. (2009). Ocean acidification: The other CO₂ problem.
740 *Annual Review of Marine Science*, 1, 169–192. <https://doi.org/10.1146/annurev.marine.010908.163834>
- 741 Driscoll, C., Driscoll, K., Roy, K., & Mitchell, M. (2003). Chemical Response of Lakes in the Adirondack Region of
742 New York to Declines in Acidic Deposition. *Environmental Science and Technology*, 37(10), 2036–2042.
743 <https://doi.org/10.1021/es020924h>
- 744 Gaillardet, J. (2018). Global climate control on carbonate weathering intensity. *Chemical Geology*.
745 <https://doi.org/10.1016/j.chemgeo.2018.05.009>
- 746 Garmo, Ø. A., Skjelkvåle, B. L., De Wit, H. A., Colombo, L., Curtis, C., Fölster, J., et al. (2014). Trends in Surface
747 Water Chemistry in Acidified Areas in Europe and North America from 1990 to 2008. *Water, Air, and Soil*
748 *Pollution*, 225, 1880. <https://doi.org/10.1007/s11270-014-1880-6>
- 749 Gelman, J., Carlin, J.B., Stern, H.S., Dunson, D.B., Vehtari, A., & Rubin, D.B. (2013) *Bayesian Data Analysis*,
750 *Third Edition*. St. Louis, MO: Chapman & Hall/CRC
- 751 Gray, N. (1997). Environmental impact and remediation of acid mine drainage: a management problem.
752 *Environmental Geology*, 30, 62–71. <https://doi.org/10.1007/s002540050133>
- 753 Grimm, N. B., Faeth, S. H., Golubiewski, N. E., Redman, C. L., Wu, J., Bai, X., & Briggs, J. M. (2008). Global
754 change and the ecology of cities. *Science*, 39(5864), 756–760. <https://doi.org/10.1126/science.1150195>
- 755 Hemingway, J.B., Olson, H., Turchyn, A.V., Tipper, E.T., Bickle, M.J., & Johnston, D.T. (2020) Triple oxygen
756 isotope insight into terrestrial pyrite oxidation. *Proceedings of the National Academy of Sciences of the United*
757 *States of America*, 117(14), 7650–7657. <https://doi.org/10.1073/pnas.1917518117>
- 758 Herlihy, A.T., Kaufmann, P.R., Mitch, M.E. et al. (1990). Regional estimates of acid mine drainage impact on
759 streams in the mid-atlantic and Southeastern United States. *Water, Air, and Soil Pollution* 50, 91–107.
760 <https://doi.org/10.1007/BF00284786>
- 761 Hirsch, R.M., & De Cicco, L. A. (2015). User guide to Exploration and Graphics for RivEr Trends (EGRET) and
762 data retrieval: R packages for hydrologic data (version 2.0, February 2015). *U.S. Geological Survey*
763 *Techniques and Methods* (Book 4, chap. A10). United States Geological Survey.
764 <https://doi.org/http://dx.doi.org/10.3133/tm4A10>
- 765 Hirsch, Robert M., Moyer, D. L., & Archfield, S. A. (2010). Weighted Regressions on Time, Discharge, and Season

- (WRTDS), with an Application to Chesapeake Bay River Inputs. *Journal of the American Water Resources Association (JAWRA)*, 46(5), 857–880. <https://doi.org/10.1111/j.1752-1688.2010.00482.x>
- International Joint Commission (IJC). (2014). *Canada-United States Air Quality Agreement Progress Report 2014*. <https://doi.org/En85-1/2014E-PDF>
- Jeffries, D.S., Lam, D. C. L., Wong, I., & Moran, M. D. (2000). Assessment of changes in lake pH in southeastern Canada arising from present levels. *Canadian Journal of Fisheries and Aquatic Sciences*, 57(S2), 40–49. <https://doi.org/10.1139/f00-128>
- Jeffries, Dean S., Brydges, T. G., Dillon, P. J., & Keller, W. (2003). Monitoring the results of Canada/U.S.A. acid rain control programs: Some Lake responses. *Environmental Monitoring and Assessment*, 88(1–3), 3–19. <https://doi.org/10.1023/A:1025563400336>
- Karberg, N.J., Pregitzer, K.S., King, J.S., Friend, A.L., & Wood, J.R. (2005). Soil carbon dioxide partial pressure and dissolved inorganic carbonate chemistry under elevated carbon dioxide and ozone. *Global Change Ecology*, 142, 296–306. <https://doi.org/10.100/s00442-004-1665-5>
- Larssen, T., Lydersen, E., Tang, D., Gai, J., Liu, H., Duan, L., et al. (2006). Acid Rain in China. *Environmental Science & Technology*, 40(2), 418–425. <https://doi.org/10.1021/es0626133>
- Lauerwald, R., Hartmann, J., Moosdorf, N., Kempe, S., & Raymond, P.A. (2013). What controls the spatial patterns of the riverine carbonate system? — A case study for North America. *Chemical Geology*, 337–338, 114–127. <https://doi.org/10.1016/j.chemgeo.2012.11.011>
- Lawrence, G. B., & Huntington, T. G. (1999). Soil-Calcium Depletion Linked To Acid Rain and Forest Growth in the Eastern United States. *Water Resources Investigation Reports*, 98(4267), 1–12. <https://doi.org/10.3133/wri984267>
- Likens, G. E., Driscoll, C. T., & Buso, D. C. (1996). Long-Term Effects of Acid Rain: Response and Recovery of a Forested Ecosystem. *Science*, 272(5259), 244–246. <https://doi.org/10.1126/science.272.5259.244>
- Likens, G.E., Bormann, F.H., & Johnson, N.M. (1972) Acid Rain. *Environment: Science and Policy for Sustainable Development*, 14(2), 33–40. <https://doi.org/10.1080/00139157.1972.9933001>
- Lu, C., & Tian, H. (2017). Global nitrogen and phosphorus fertilizer use for agriculture production in the past half century: Shifted hot spots and nutrient imbalance. *Earth System Science Data*, 9, 181–192. <https://doi.org/10.5194/essd-9-181-2017>

- Majer, V., Krám, P., & Shanley, J. B. (2005). Rapid regional recovery from sulfate and nitrate pollution in streams of the western Czech Republic - comparison to other recovering areas. *Environmental Pollution*, 135(1), 17–28. <https://doi.org/10.1016/j.envpol.2004.10.009>
- Martin, J.B. (2017). Carbonate minerals in the global carbon cycle. *Chemical Geology*, 449, 58-72. <https://doi.org/10.1016/j.chemgeo.2016.11.029>
- Marx, A., Hintze, S., Sanda, M., Jankovec, J., Oulehle, F., Dusek, J. et al. (2017). Acid rain footprint three decades after peak deposition: Long-term recovery from pollutant sulphate in the Uhlirská catchment (Czech Republic). *Science of the Total Environment*, 598, 1037–1049. <https://doi.org/10.1016/j.scitotenv.2017.04.109>
- McHale, M. R., Burns, D. A., Siemion, J., & Antidormi, M. R. (2017). The response of soil and stream chemistry to decreases in acid deposition in the Catskill Mountains, New York, USA. *Environmental Pollution*, 229, 607–620. <https://doi.org/10.1016/j.envpol.2017.06.001>
- Menz, F. C., & Seip, H. M. (2004). Acid rain in Europe and the United States: An Update. *Environmental Science and Policy*, 7, 253–265. <https://doi.org/10.1016/j.envsci.2004.05.005>
- Moosdorf, N., Hartmann, J., & Dürr, H.H. (2010). Lithological composition of the North American continent and implications of lithological map resolution for dissolved silica flux modeling. *Geochemistry, Geophysics, Geosystems*, 11(11), 1-18. <https://doi.org/10.1029/2010GC003259>
- Mosley, L., Zammit, B., Jolley, A., & Barnett, L. (2014). Acidification of lake water due to drought. *Journal of Hydrology*, 511, 484-493. <https://doi.org/10.1016/j.jhydrol.2014.02.001>
- Murphy, J., Hirsch, R., & Sprague, L. (2013). Nitrate in the Mississippi River and its tributaries, 1980–2010—An update. *U.S. Geological Survey Scientific Investigations Report*, 2013(5159), 1–31. <https://doi.org/http://pubs.usgs.gov/sir/2013/5169/>
- National Atmospheric Deposition Program (NADP) (NRSP-3). (2020). *NADP Program Office, Wisconsin State Laboratory of Hygiene*, 465 Henry Mall, Madison, WI 53706.
- Neal, C., & Whitehead, P. G. (1988). The role of CO₂ in long term stream acidification processes: A modelling viewpoint. *Hydrological Sciences Journal*, 33(1), 103–108. <https://doi.org/10.1080/02626668809491225>
- Nordstrom, D. K. (2000). Advances in the Hydrogeochemistry and Microbiology of Acid Mine Waters. *International Geology Review*, 42(6), 499-515. doi:10.1080/00206810009465095
- Perrin, A. S., Probst, A., & Probst, J. L. (2008). Impact of nitrogenous fertilizers on carbonate dissolution in small

- agricultural catchments: Implications for weathering CO₂ uptake at regional and global scales. *Geochimica et Cosmochimica Acta*, 72(2008), 3105–3123. <https://doi.org/10.1016/j.gca.2008.04.011>
- Plummer, M. (2019). rjags: Bayesian Graphical Models using MCMC. R package version 4-10. <https://CRAN.R-project.org/package=rjags>
- Potter, P., Ramankutty, N., Bennett, E.M., & Donner, S.D. (2010). Characterizing the Spatial Patterns of Global Fertilizer Application and Manure Production. *Earth Interactions*, 14(2), 1-22. <https://doi.org/10.1175/2009EI288.1>
- Rabalais, N. N., Turner, R. E., Díaz, R. J., & Justić, D. (2009). Global change and eutrophication of coastal waters. *ICES Journal of Marine Science*, 66(7), 1528–1537. <https://doi.org/10.1093/icesjms/fsp047>
- Raymond, P.A., & Cole, J.J. (2003). Increase in the export of alkalinity from North America's largest river. *Science*, 301(5629), 88-91. <https://doi.org/10.1126/science.1083788>
- Raymond, P.A., Hartmann, J., Lauerwald, R., Sobek, S., McDonald, C., Hoover, M., Butman, D., Striegl, R., Mayorga, E. & Humborg, C. (2013). Global carbon dioxide emissions from inland waters. *Nature*, 503(7476), 355-359. <https://doi.org/10.1038/nature12760>
- Raymond, P. A., & Oh, N. (2009). Long term changes of chemical weathering products in rivers heavily impacted from acid mine drainage: Insights on the impact of coal mining on regional and global carbon and sulfur budgets. *Earth and Planetary Science Letters*, 284(1-2), 50-56. <https://doi.org/10.1016/j.epsl.2009.04.006>
- Reddy, M. M., Sherwood, S. I., & Doe, B. R. (1986). Limestone and Marble Dissolution by Acid Rain: An Onsite Weathering Experiment. In *American Chemical Society* (pp. 226–238). <https://doi.org/10.1021/bk-1986-0318.ch015>
- Reiman, J. H., & Xu, Y. J. (2019). Diel variability of pCO₂ and CO₂ outgassing from the Lower Mississippi River: Implications for riverine CO₂ outgassing estimation. *Water*, 11(43), 1–15. <https://doi.org/10.3390/w11010043>
- Rice, K. C., Scanlon, T. M., Lynch, J. A., & Cosby, B. J. (2014). Decreased Atmospheric Sulfur Deposition across the Southeastern U.S.: When Will Watersheds Release Stored Sulfate? *Environmental Science and Technology*, 48, 10071–10078. <https://doi.org/10.1021/es501579s>
- Skjelkvåle, B. L., Jeffries, D. S., Stoddard, J. L., Kemp, A., Lükewille, A., Stainton, M. P., et al. (2002). Regional trends in aquatic recovery from acidification in North America and Europe. *Nature*, 401(6753), 575–578. <https://doi.org/10.1038/44114>

- 850 Song, C., Liu, C., Han, G., & Liu, C. (2017). Impact of different fertilizers on carbonate weathering in a typical karst
851 area, Southwest China: A field column experiment. *Earth Surface Dynamics*, 5(3), 605–616.
852 <https://doi.org/10.5194/esurf-5-605-2017>
- 853 Stets, E. G., Kelly, V. J., & Crawford, C. G. (2014). Long-term trends in alkalinity in large rivers of the
854 conterminous US in relation to acidification, agriculture, and hydrologic modification. *Science of the Total*
855 *Environment*, 488–489, 280–289. <https://doi.org/10.1016/j.scitotenv.2014.04.054>
- 856 Stoddard, J. L., Jeffries, D. S., Lükewille, A., Kemp, A., Stainton, M. P., Traaen, T., et al. (1999). Regional trends in
857 aquatic recovery from acidification in North America and Europe. *Nature*, 401, 575–578.
858 <https://doi.org/10.1038/44114>
- 859 Tans, P., & Keeling, R. (2020). Mauna Loa CO₂ Annual Mean Data. *NOAA/GML and Scripps Institution of*
860 *Oceanography*. Received May 15, 2020, from <https://www.esrl.noaa.gov/gmd/ccgg/trends/data.html>
- 861 Thomson, C. J., Marschner, H., & Römhild, V. (1993). Effect of nitrogen fertilizer form on pH of the bulk soil and
862 rhizosphere, and on the growth, phosphorus, and micronutrient uptake of bean. *Journal of Plant Nutrition*,
863 16(3), 493–506. <https://doi.org/10.1080/01904169309364548>
- 864 Thrash, J. C., Seitz, K. W., Baker, B. J., Temperton, B., Gillies, L. E., Rabalais, N. N., et al. (2017). Metabolic Roles
865 of Uncultivated Bacterioplankton Lineages in the Northern Gulf of Mexico “Dead Zone.” *MBio*, 8(5), 1–20.
866 <https://doi.org/10.1128/mBio.01017-17>
- 867 Todd, A.S., Manning, A.H., Verplanck, P.L., Crouch, C., McKnight, D.M., & Dunham, R. (2012). Climate-Change-
868 Driven Deterioration of Water Quality in a Mineralized Watershed. *Environmental Science and Technology*,
869 46, 9324–9332. <https://doi.org/10.1021/es3020056>
- 870 U.S. Department of Agriculture National Agricultural Statistics Service Cropland Data Layer (CDL) (2020).
871 Published crop-specific data layer [Online]. Available at <http://nassgeodata.gmu.edu/CropScape/> (accessed
872 May 15 2020; verified May 15 2020). USDA-NASS, Washington, DC.
- 873 U.S. Energy Information Administration. (2017). Annual Survey of Coal Production and Preparation, Form EIA-7A.
874 Accessed January, 21, 2021.
- 875 U.S. Geological Survey. (2020). National Water Information System data available on the World Wide Web (USGS
876 Water Data for the Nation), accessed [2017], at URL [<http://waterdata.usgs.gov/nwis/>].
877 <http://dx.doi.org/10.5066/F7P55KJN>

- van Vliet, M.T.H., & Zwolsman, J.J.G. (2008) Impact of summer droughts on the water quality of the Meuse River. *Journal of Hydrology*, 353, 1-17. <https://doi.org/10.1016/j.jhydrol.2008.01.001>
- Waller, K., Driscoll, C., Lynch, J., Newcomb, D., & Roy, K. (2012). Long-term recovery of lakes in the Adirondack region of New York to decreases in acidic deposition. *Atmospheric Environment*, 46, 56–64. <https://doi.org/10.1016/j.atmosenv.2011.10.031>
- Walna, B., Drzymala, S., & Siepak, J. (1998). The impact of acid rain on calcium and magnesium status in typical soils of the Wielkopolski National Park. *Science of the Total Environment*, 220(2–3), 115–120. [https://doi.org/10.1016/S0048-9697\(98\)00240-X](https://doi.org/10.1016/S0048-9697(98)00240-X)
- Weary, D. J., & Doctor, D. H. (2014). Karst in the United States: A digital map compilation and database. *United States Geological Survey Open-File Report*, 1156, 23. <http://dx.doi.org/10.3133/ofr20141156>
- Westmacott, J.R., & Burn, D.H. (1997). Climate change effects on the hydrologic regime within the Churchill-Nelson River Basin. *Journal of Hydrology*, 202(1-4), 263-279. [https://doi.org/10.1016/S0022-1694\(97\)00073-5](https://doi.org/10.1016/S0022-1694(97)00073-5)
- Wisniewski, J., & Keitz, E.L. (1983) Acid Rain Deposition Patterns in the Continental United States. *Water, Air and Soil Pollution*, 19, 327-339. <https://doi.org/10.1007/BF00159594>
- Zhi, W., Li, L., Dong, W., Brown, W., Kaye, J., Steefel, C., & Williams, K.H. (2019). Distinct Source Water Chemistry Shapes Contrasting Concentration-Discharge Patterns. *Water Resources Research*, 55(5), 4233-4251. <https://doi.org/10.1029/2018WR024257>